

INVITED FEATURE SECTION

Hepatocellular nodules in liver cirrhosis: state of the art CT evaluation (perfusion CT/volume helical shuttle scan/dual-energy CT, etc.)

Masahiro Okada,¹ Tonsok Kim,² Takamichi Murakami¹

¹Department of Radiology, Kinki University School of Medicine, 377-2 Ohno-Higashi, Osaka-Sayama, Osaka 589-8511, Japan

²Department of Radiology, Osaka University Graduate School of Medicine, 2-2 Yamadaoka, Suita, Osaka 565-0871, Japan

Abstract

The purpose of this article is to explain the role of advanced liver CT imaging, including perfusion CT, dual-energy CT, and volume helical shuttle (VHS) scanning, with regard to its clinical applications. Perfusion CT is a promising method for calculating hepatic blood flow and portal blood flow, including microcirculation, using a color-encoded display of parameters obtained from the liver time–density curve, with iodine contrast agent. Tumor angiogenesis and assessment of the response to antiangiogenesis treatment (e.g., Sorafenib) can be analyzed by perfusion CT of the liver. VHS scan has very high temporal resolution due to the reciprocating movement employed during scanning, enabling the acquisition of 24 scans of the whole liver in the arterial dominant phase during a 40-s breath hold, and a reduction in radiation dose. Dual-energy CT enables differentiation of materials and tissues based on their CT density values, using two different energy spectra. This method includes a low tube voltage CT technique that increases the contrast enhancement of vascular structures while simultaneously reducing radiation dose. Images obtained at the preferred settings of low tube voltage and high tube current, with dose reduction in the hepatic arterial phase, are useful for detecting hypervascular hepatocellular carcinoma.

Key words: Perfusion—Dual energy—Computed tomography—Shuttle helical scan—Hepatocellular carcinoma

This article focuses on the interpretation of new practical development in computed tomography (CT). In liver imaging, diagnostic accuracy, potential pitfall and limitation by perfusion CT, dual-energy CT, and volume shuttle helical scan are addressed. And dose reduction with these new CT technologies is also addressed.

Perfusion CT

CT can be used not only to image anatomical structure, but also to analyze liver function. Perfusion CT is performed by the acquisition of serial images after the administration of a bolus of iodinated contrast agent, enabling detailed analysis of liver hemodynamics. This CT technique is designed to calculate hepatic blood flow and portal blood flow using a color-encoded display of parameters from the liver time–density curve (TDC), with iodine contrast agent. Thus, liver functional maps are calculated by the input function based on regions of interest (ROIs) set on the aorta and portal vein.

Sahani et al. [1] reported perfusion CT as a feasible technique for quantifying tumor vascularity and angiogenesis in advanced HCC. Perfusion CT is obtained by monitoring the first pass through the vasculature after bolus injection of an iodinated contrast agent, and depicts tumor vascular physiology in patients with HCC. Following advances in imaging techniques and post-processing software, a deconvolution-based method has become widely used for liver perfusion CT imaging [2, 3]. There are two vascular inputs (hepatic arterial flow and portal flow) to the liver; however, the deconvolution-based method enables analysis of liver perfusion on CT. Enhancement of the abdominal aorta is used as a substitute for hepatic artery input, because the hepatic artery is too small to obtain a reliable TDC.

Hepatic perfusion CT enables analysis of liver function, and measurement of the following: tissue blood flow (TBF; mL/min/100 g); tissue blood volume (TBV; mL/100 g); mean transit time (MTT; s), which is the average time for blood elements to traverse the vasculature from arterial inlet to venous outlet (proportional to perfusion pressure); and hepatic arterial fraction (HAF; %), which is the ratio of arterial perfusion to total liver perfusion. The passage of contrast material through blood vessels enables the calculation of a TDC. The impulse residue function (IRF) of a localized bolus in hepatic blood flow is fundamental to perfusion CT. The passage of contrast agent enables the calculation of a TDC, and is shown as the IRF.

Mathematically, IRF is calculated as a tissue curve. This principle is shown as follows: [3].

$$Q(t) = \text{TBF} \times I(t) \int R(t)$$

$$I(t) = \alpha \text{Ca}(t) + (1 - \alpha) \text{Cp}(t)$$

where $Q(t)$, TDC in the liver; TBF, tissue blood flow; $I(t)$, iodine concentration flowing through the liver; \int , convolution; $R(t)$, impulse residue function; α , hepatic arterial fraction (HAF); $\text{Ca}(t)$, iodine concentration of hepatic artery; $\text{Cp}(t)$, concentration of contrast medium of portal vein.

Positron emission tomography (PET) also provides information regarding tissue perfusion, including that of the liver, but the spatial resolution is low [4]. The application of MRI is limited because of difficulty in quantifying the concentration of contrast agent in the tissue and its high sensitivity to respiratory movement [5, 6].

Xenon CT, which was developed during the late 1970s and 1980s, has been used to obtain information on cerebral blood flow following the inhalation of non-radioactive xenon gas [7, 8]. Xenon CT enables quantitative evaluation of hepatic arterial and portal-venous blood flow [9–11]; however, specialized equipment is required. Hashimoto et al. [12] reported a good correlation between hepatic TBF quantified by xenon CT and that by perfusion CT with iodine. In the clinical setting, perfusion CT has greater availability than xenon CT because dynamic CT with iodine is an established method for investigating liver tumors.

Clinical impact of hepatic perfusion CT

Analysis of the microcirculation by perfusion CT may be useful in the clinical situation; e.g., in the evaluation of response to therapy. Perfusion CT can be used for detection of tumor angiogenesis and in assessing response to antiangiogenic treatment for various cancers [13–16]. The greatest impact of perfusion CT with regard to the liver is in assessment of patients with HCC, especially that of tumor response to antiangiogenic drugs [17, 18].

Standard chemotherapy is not a treatment method for advanced HCC because of its chemo-resistance. Sorafenib (Nexavar®, Bayer Schering Pharma AG, Berlin, Germany), an orally active multikinase inhibitor with effects on tumor-cell proliferation and tumor angiogenesis, is a promising therapy that demonstrates superior survival in advanced HCC [19]. Therapeutic response has been assessed based on tumor size measurement using the Response Evaluation Criteria in Solid Tumors (RECIST). This assessment for response to Sorafenib therapy by RECIST, however, has highlighted the limitations associated with morphologic measurement. Perfusion CT quantifies not only tumor biologic behavior, but also changes in liver parenchyma (without tumor) caused by Sorafenib therapy in patients with advanced HCC (Figs. 1, 2).

For detecting and characterizing hepatic tumors in the clinical setting, perfusion CT can be followed by liver dynamic CT. Tissue enhancement curves can be mathematically fitted to a compartmental or deconvolution model, and quantitative parameters such as TBV, TBF, MTT, and HAF can be obtained. The linearity between tissue attenuation and iodine concentration contributes to the estimation of quantitative parameters.

Liver perfusion CT has generally been performed for a single section [12, 20, 21]; however, the high temporal resolution of volume helical shuttle (VHS) scanning enables whole liver perfusion imaging with multi-sections.

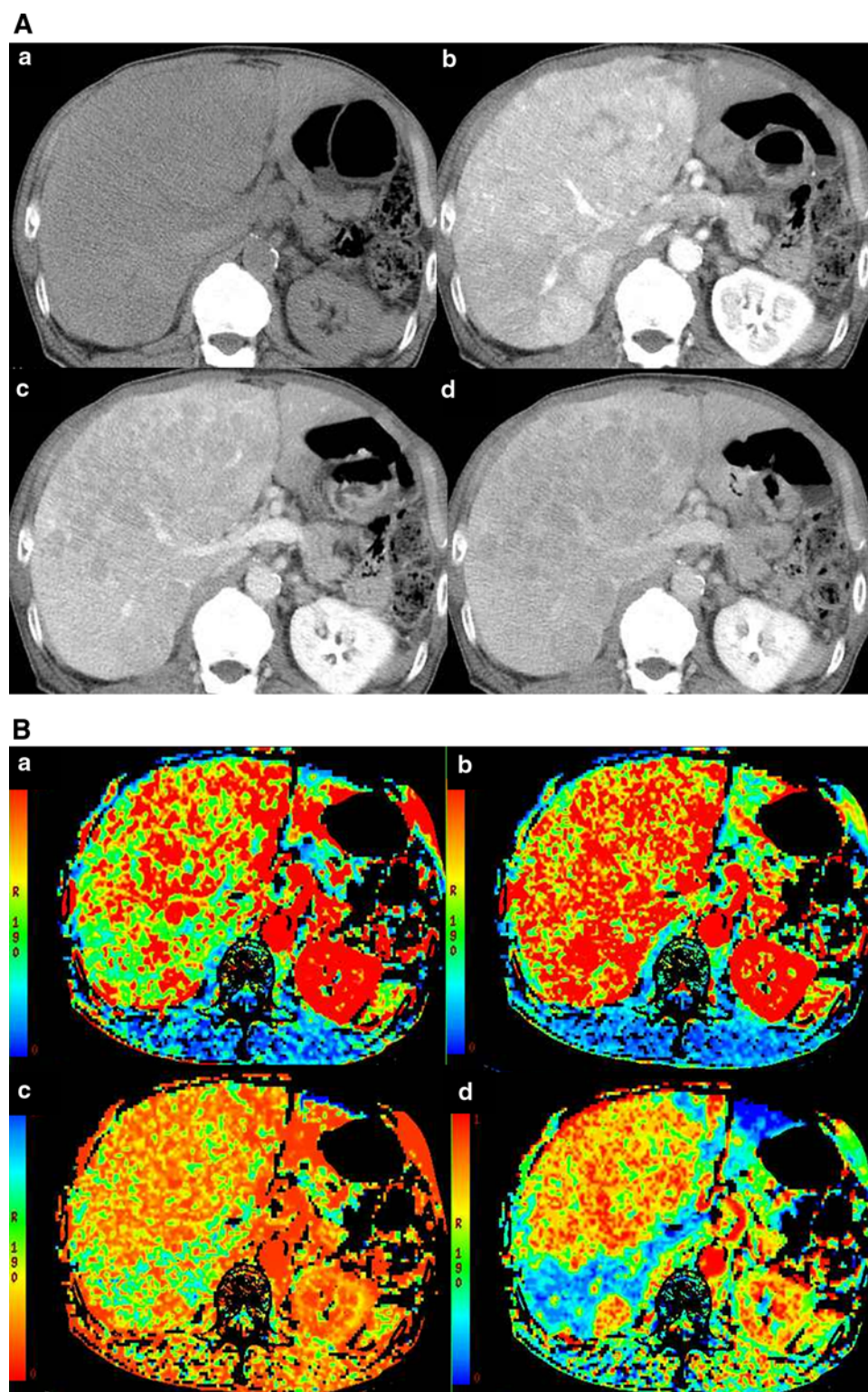
Liver cirrhosis and perfusion CT

Hepatic arterial perfusion is increased in patients with cirrhosis [21, 22]. Hashimoto et al. [21] reported the mean TBF, TBV, MTT, and HAF values of normal subjects by a deconvolution algorithm to be 103.9 ± 18 mL/min/100 g, 12.5 ± 2.0 mL/100 g, 11.1 ± 1.6 s, and $18.4 \pm 5.6\%$, respectively. In contrast, the mean TBFs of patients with Child A, B, and C were 95.1 ± 24 , 86.7 ± 29 , and 75.5 ± 6.5 mL/min/100 g, respectively. Bader et al. investigated perfusion CT using a maximum gradient algorithm. The comparison between a deconvolution algorithm and a maximum gradient algorithm in perfusion CT of normal subjects is shown in Table 1. Evaluation of local liver function by perfusion CT may be important in some clinical situations, such as planning of surgery and therapy evaluation.

Limitations and solutions for perfusion CT

Perfusion CT has the major drawback of radiation exposure, but Adaptive Statistical iterative Reconstruction (ASiR, GE Healthcare, Milwaukee, WI, USA) provides similar quality at lower dose compared with the usual filtered back-projection algorithm. If ASiR is used at the same dose, better image quality is obtained than that using the back-projection algorithm.

Fig. 1. A 60-year-old man with an advanced hepatocellular carcinoma (HCC). **A** Advanced HCC pre-Sorafenib-therapy on dynamic CT. **a** Pre-enhancement CT, **b** arterial phase, **c** portal phase, **d** equilibrium phase. Dynamic liver CT showed the large HCC with hypervascularity at the arterial phase (**a**) and washout at the equilibrium phase (**d**) in right lobe and segment 4 of the liver. **B** Advanced HCC pre-Sorafenib-therapy on perfusion CT. **a** Tissue blood flow (TBF; mL/min/100 g), **b** tissue blood volume (TBV; mL/100 g), **c** mean transit time (MTT; s), **d** hepatic arterial fraction (HAF; %). Each parameter of HCC and liver parenchyma was TBF; 297, TBV; 28, MTT; 43, HAF; 80 and TBF; 179, TBV; 27, MTT; 12, HAF; 17, respectively. This case suggests the ability of perfusion CT to demonstrate advanced hypervascular HCC and liver parenchyma.

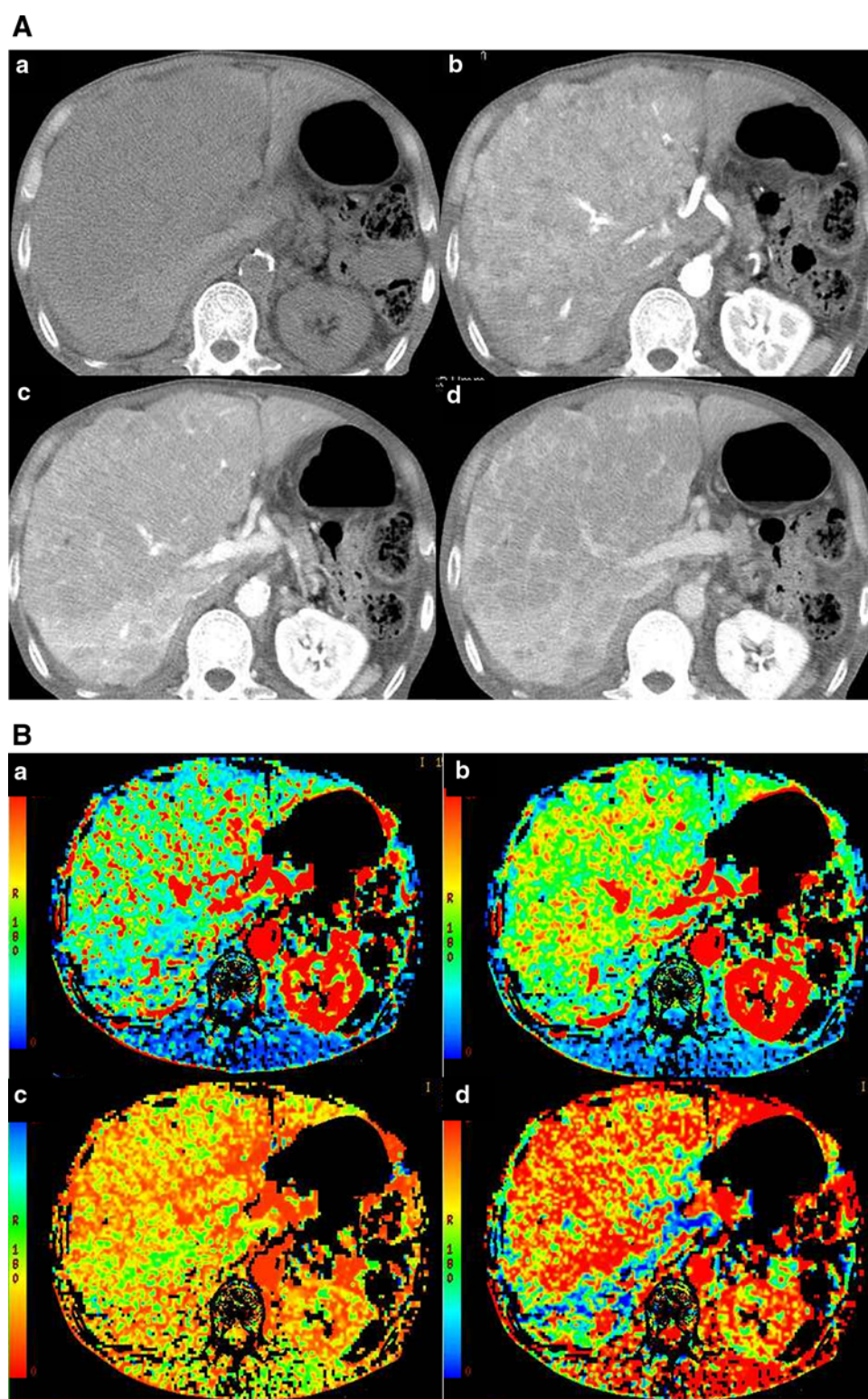


Perfusion CT has a limitation when scanning small targets because the obtained color-mapping image may not enable visualization of a small lesion. This limits the number of such studies permissible in the course of a clinical trial; however, implementation of low-dose scanning protocols may lead to more widespread and frequent use of this technique.

VHS

The VHS technique is a breakthrough technique for liver imaging that offers new clinical opportunities such as dynamic blood flow studies, leading to a new concept termed “four-dimensional (4D) CT.” In addition, when VHS is used with ASiR, the acquired images can be

Fig. 2. A 60-year-old man with an advanced hepatocellular carcinoma (HCC). **A** Advanced HCC post-Sorafenib-therapy (4 months) on dynamic CT. **a** Pre-enhancement CT, **b** arterial phase, **c** portal phase, **d** equilibrium phase. Early enhancement of large HCC in right lobe and segment 4 of the liver at the arterial phase (**a**) decreased after Sorafenib therapy, in comparison to pre-therapy (Fig. 1A). **B** Advanced HCC post-Sorafenib-therapy (4 months) on perfusion CT. **a** Tissue blood flow (TBF; mL/min/100 g), **b** tissue blood volume (TBV; mL/100 g), **c** mean transit time (MTT; s), **d** hepatic arterial fraction (HAF; %). Each parameter of HCC and liver parenchyma was TBF; 152, TBV; 14, MTT; 7, HAF; 87 and TBF; 84, TBV; 15, MTT; 16, HAF; 9, respectively. The decreases of TBV and TBF of HCC after Sorafenib therapy reflected antiangiogenic response, and was TBV of HCC was correlated with degree of arterial enhancement in liver dynamic CT.



produced without artifacts. ASiR enables a reduction in radiation dose compared with the usual filtered back-projection algorithm; alternatively, when employed at the same dose as that for the filtered back-projection algorithm, ASiR provides better image quality. We performed the world's first VHS CT scan for dynamic CT

angiography and also for liver- and brain-perfusion studies, with high temporal resolution. VHS provides almost real-time hemodynamic change by shuttling the CT scanning cradle back and forth during scanning, and also enables wider coverage for complete organ imaging: >120 mm longitudinally. In contrast, conventional

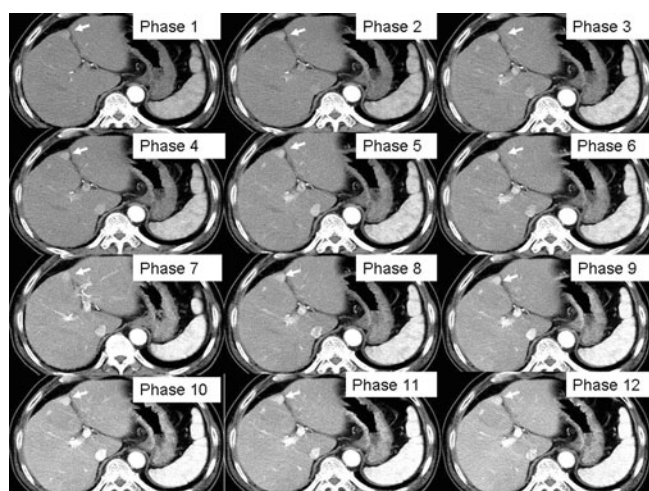


Fig. 3. A 50-year-old man with a small hypervascular hepatocellular carcinoma (HCC). Volume helical shuttle (VHS) scan was performed at 12 phases in the arterial phase of dynamic CT. Arterial enhancement pattern of HCC (arrow) in liver segment 4 was analyzed in detail.

helical scans are performed at a constant table speed, meaning that the exposure is ineffective during acceleration of the table, and temporal resolution of conventional helical scan is lower than that of VHS.

The VHS technique requires no extra exposure because the acquisition of CT data is effective even with varying table speed. **The whole liver can be scanned 24 times (12 round trips) during a 40-s breath hold, enabling the technique to be used for perfusion CT.** Because VHS is a fast scanning technique (e.g., approximately 2 s/whole liver scan) with improved temporal resolution, even during table acceleration/deceleration; therefore, it can be used to investigate the relation between tumors and feeding arteries in detail. VHS could possibly be used as a navigation tool for therapy, such as transarterial chemoembolization (TACE) in HCCs; it could also be used to perform physiological assessment of the liver.

VHS has potential for use in 4D imaging; that is, producing a movie-like image, with a wide volume coverage. With VHS, the liver is repeatedly scanned in axial acquisitions, thereby providing coverage of the whole liver with reciprocating movement. Hypervascular HCC can be analyzed by using several whole liver scans, such as 12 phases in the arterial phase of dynamic CT (Fig. 3).

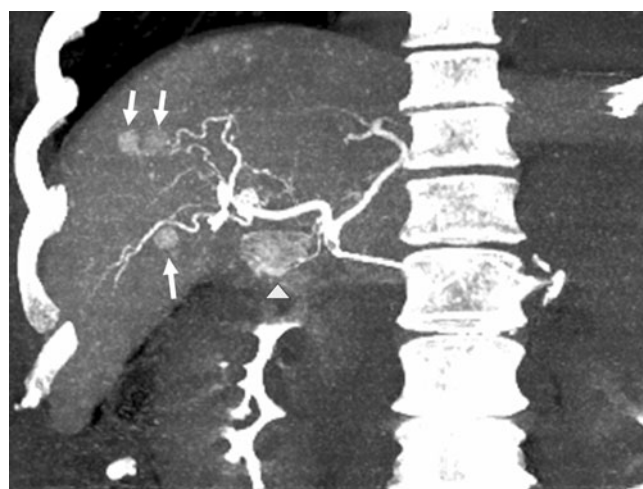


Fig. 4. A 60-year-old man with multiple hypervascular hepatocellular carcinomas (HCCs). The VHS technique can be used for four-dimensional (4D) CT angiography. This image was obtained at a coronal plane. When used with CT angiography, the hepatic arteries and multiple HCCs (arrows) could be visualized to almost the same degree as with conventional digital subtraction angiography (DSA) examination. Arrow head shows stain of the gallbladder.

Blood flow information, such as a blood flow direction, can also be obtained by VHS scanning.

The VHS technique can be used for perfusion studies of the liver and for 4D CT angiography. When used with CT angiography, the main abdominal vessels can be visualized to almost the same degree as with conventional digital subtraction angiography (DSA) (Fig. 4).

Dual-energy CT

Dual-energy CT is a promising technique used to obtain material-specific images. It enables differentiation of materials and tissues in images obtained based on the differences in iodine and water densities; the resulting CT images are reconstructed using two different energy spectra. Techniques based on the concept of dual-energy have been explored over the past 30 years [23]. Dual-energy CT can be performed with multidetector CT (e.g., 64-detector row CT) in current clinical settings.

An advantage of dual-energy CT is its ability to perform scanning at low tube voltages (kVp). Because of the photoelectric effect, the attenuation value of iodine is

Table 1. Comparison between two perfusion CTs in normal subjects

	TBF	HAP	PVP	HAF
Hashimoto et al.	103.9 ± 18	19.0 ± 7.8	83.0 ± 14.0	18.4 ± 5.6
Bader et al.	138.0 ± 32	16.0 ± 6.0	122.0 ± 29.0	12.0 ± 3.0

Note: Hashimoto et al. [12, 21] calculated by using a deconvolution algorithm, Bader et al. [20] calculated by using a maximum gradient algorithm. Data are shown as mean ± SD

TBF hepatic tissue blood flow (mL/min/100 g), HAP hepatic arterial perfusion (mL/min/100 g), PVP portal-venous perfusion (mL/min/100 g), HAF hepatic arterial fraction (%)

higher when low-voltage X-rays (such as 80 kVp) are used [24, 25]. Iodine contrast agents are more conspicuous at low than at high tube voltage settings, but may result in high image noise, particularly in large patients [26]. The increased noise of low-voltage X-ray scanning may be problematic because the density of the liver is relatively homogeneous. Therefore, maintaining an appropriate signal-to-noise ratio (SNR) in low-voltage raw data is an important factor in dual-energy scanning.

There are four types of dual-energy CT systems, although two of these have only recently become commercially available. These dual-energy techniques are used routinely in clinical abdominal imaging.

GE Healthcare incorporates two advanced technologies for dual-energy CT: a gemstone detector in the scanner, which uses a garnet-based detector material; and fast kV switching, in which the kVp levels are switched with every other view. Gemstone spectral imaging is designed to reduce afterglow in the detectors. Intermittently and alternately, 80 and 140 kVp X-rays change for each view during fast kV switching. Only one X-ray tube is used instead of two, which produces X-rays at two different energies (80 and 140 kVp) in alternative views; thus, dual-energy CT can be performed with “projection base” dual-energy reconstruction with beam-hardening reduction, to produce monochromatic images. This fast kV switching method requires specialized technology to control the high frequency and high voltage of the high voltage generator. Without this technology, dual-energy scanning is disadvantaged by limited energy separation.

The Siemens dual-energy CT technique has two X-ray sources and two X-ray detectors offset by 90°, with a single CT gantry. This system has the advantage of better energy separation compared with the fast kV switching method; however, the dual-source CT system has the disadvantage of cross-contamination by scattering, and “image base” dual-energy reconstruction is performed without beam-hardening reduction. Thus, the lower-energy blended images exhibit a greater beam-hardening effect compared with that for other techniques.

Philips and Toshiba employ a slow kV switching system for dual-energy CT at alternative rotation, although this system is not commercially available. Slow kV switching has the advantage of better energy separation compared with other methods, but has the disadvantage of difficulty in performing helical scans because of the alternating rotations of the X-ray tube, as well as problems concerning patient misregistration artifact.

Several previous studies have employed dual-energy CT for clinical use in the abdominal region [27–29]. Dual-energy CT provides an accurate, noninvasive method of quantitating liver iron [30], offers more specific tissue characterization on CT, and can improve the assessment of vascular disease [31] (Fig. 5A). Dual-energy CT has been shown to have improved ability to detect contrast agent and to distinguish high-density

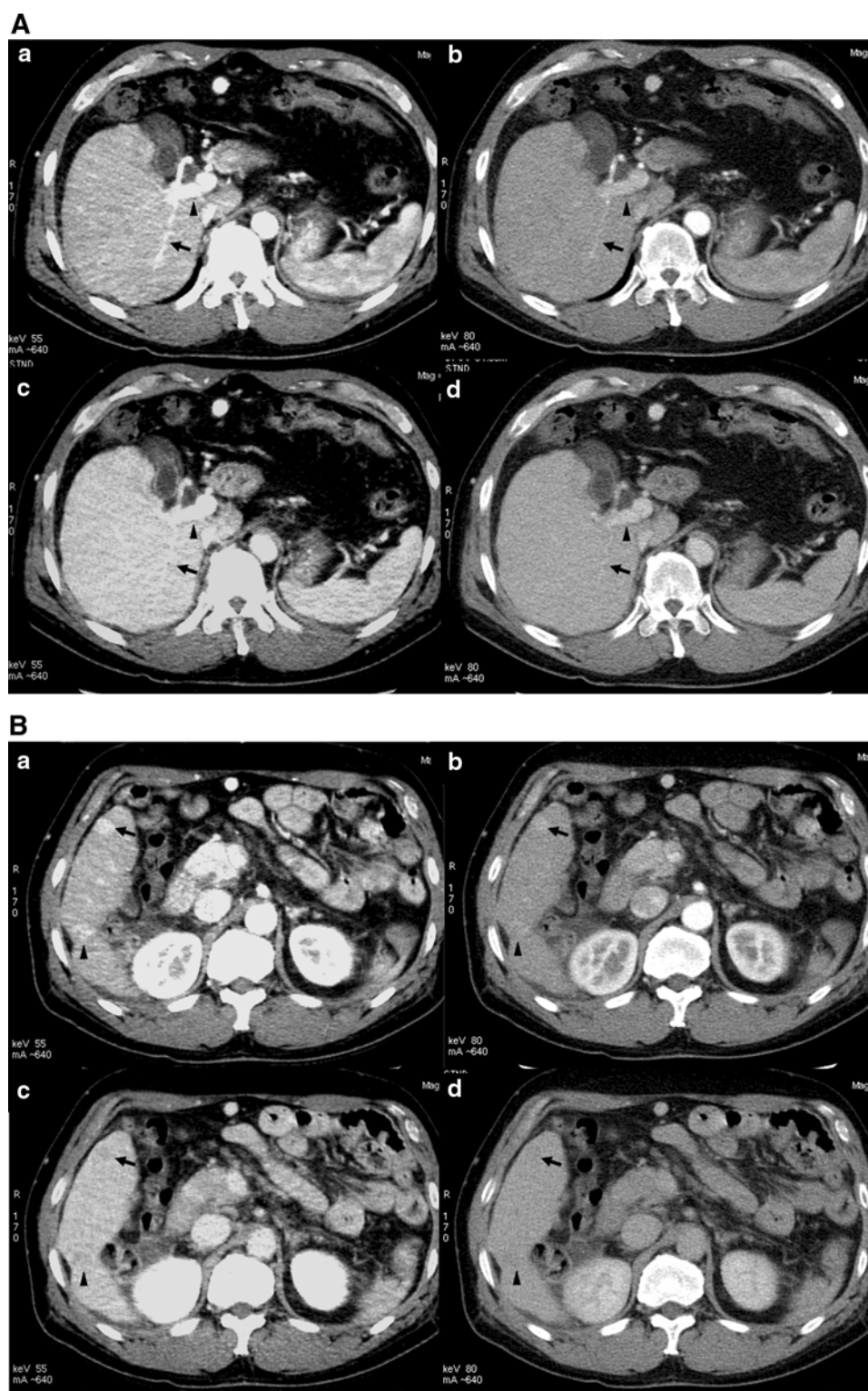
Fig. 5. A 60-year-old man with dual-energy CT imaging for hepatic vessels and two hepatocellular carcinomas (HCCs). **A** Assessment of hepatic vessels by dual-energy CT: monochromatic images with 55 keV (low tube voltage) and 80 keV (conventional tube voltage) in the arterial phase and the portal-venous phase of dynamic CT. **a** Arterial phase with 55 keV, **b** arterial phase with 80 keV, **c** portal-venous phase with 55 keV, **d** portal-venous phase with 80 keV. All images were obtained as matrix 512 × 512, 640 mA and 5 mm slice thickness. **a–d** Enhancement effects of hepatic artery (arrow) and portal vein (arrow head) with 55 keV were higher than those with 80 keV in both the arterial phase and the portal-venous phase of dynamic CT. **B** Assessment of HCC by dual-energy CT: monochromatic images with 55 keV (low tube voltage) and 80 keV (conventional tube voltage) in the arterial phase and the equilibrium phase of dynamic CT. **a** Arterial phase with 55 keV, **b** arterial phase with 80 keV, **c** equilibrium phase with 55 keV, **d** equilibrium phase with 80 keV. All images were obtained as matrix 512 × 512, 640 mA and 5 mm slice thickness. **a, b** Enhancement effects of hypervascular HCCs in liver segment 5 (arrow) and 6 (arrow head) with 55 keV were higher than those with 80 keV in the arterial phase of dynamic CT. **c, d** Equilibrium phase of dynamic liver CT showed washout (defined as low density relative to surrounding liver parenchyma) of HCCs in liver segment 5 (arrow) and 6 (arrow head). The contrast between HCC and liver parenchyma on the low tube voltage (55 keV) image was visually higher than that on the conventional tube voltage (80 keV) image.

substances created by iodine from those created by calcium or other substances, and thus is useful for the detection and characterization of renal stones [32]. Moreover, postprocessing algorithms enable subtraction of iodine maps from dual-energy CT data (e.g., subtraction of calcification) to create a virtual noncontrast image. This method may increase diagnostic accuracy, especially for detecting renal stones from the enhanced CT data alone.

Fused images can be created for dual-energy CT by using a weighting factor or the blending method for contrast enhancement [33, 34], or monochromatic images can be reconstructed by dual-energy reconstruction. Blended or monochromatic images provide some improvement in contrast. Dual-energy material decomposition images can be successfully used for routine abdominal imaging: they offer improved visualization of vascular structures and abnormal calcifications such as renal and gall stones as well as depiction of soft tissue structures such as the kidneys, liver, and spleen. Material decomposition images have the potential to increase sensitivity and specificity in the detection of pathology.

HCC diagnosis by dual-energy CT

CT images at 80 kVp or the equivalent 55 keV (kilo-electron voltage) monochromatic images may show a higher contrast-to-noise ratio for hypervascular HCCs



because the attenuation value of iodine increases with the use of low-voltage X-rays [35]. Pure 80 kVp data acquired from a dual-energy CT scanner produce greater differences in attenuation between hepatic lesions and surrounding liver, and potentially improve the

assessment and detection of liver tumors. Finally, by utilizing a dual-energy CT system with dual-energy scanning, there exists the potential to improve the assessment of hypervascular liver tumors on lower keV monochromatic images (Fig. 5B).

Dose reduction

CT image quality is strongly proportional to radiation dose. The dose level should be known when CT scanning is performed. Several parameters, such as milli-ampere (mA), exposure time, peak kilo-voltage (kVp), and pitch, are adjusted based on the relation between the benefit and risk to patients. In general, CT characteristics are largely determined by peak tube voltage (kVp), which determines the upper limit of X-ray energy, and tube current (mA). Images obtained with low-voltage X-rays contain a high degree of noise, although this is alleviated by increasing the tube current. Beam-hardening artifact is greater on low-voltage than on 120 kVp X-ray images, so a technique with reduced beam hardening in the images is desirable, such as monochromatic images made by dual-energy scanning.

Conclusion

This article summarizes the current and potential applications for perfusion CT, dual-energy CT, and VHS. CT is a powerful tool for measuring bodily architecture and function. Perfusion CT offers functional imaging that can produce important data regarding blood flow, permeability, leakage space, and blood volume. Thus, perfusion CT is feasible for monitoring the response after antiangiogenic therapy, such as Sorafenib therapy.

The VHS technique can image dynamic blood flow, leading to the new concept of four-dimensional CT, which is a movie-like image with a large volume of coverage. It also provides blood flow information, such as blood flow direction. Therefore, this technique is particularly useful for obtaining information regarding back-flow in patients with vascular stenosis or occlusion.

Dual-energy CT may offer increased detection of hepatic lesions and specific characterization in the abdominal region, and can improve the assessment of vascular disease. The study of dual-energy technology has just started in clinical settings, therefore, this technique requires extensive studies for the confirmation of clinical usefulness.

Optimization of imaging protocols for perfusion CT, dual-energy CT, and VHS can improve the utility of these techniques. In particular, low-dose CT technique is required for functional imaging, when several scans of the target lesion and organ are performed. In the future, it will be necessary to reduce the radiation dose level of abdominal CT imaging for a variety of diagnostic purposes, although new advanced technologies enable larger volumetric datasets and promising functional data to be obtained using CT.

Acknowledgments. We thank Masayuki Kudo, Akihiko Nishide, Akira Hagiwara of GE Healthcare for the advice of volume helical shuttle scan and dual-energy CT, and Takahiro Tsuboyama, MD and Masatoshi Hori, MD, PhD of Department of Radiology in Osaka University School of Medicine for data sampling.

References

1. Sahani DV, Holalkere NS, Mueller PR, Zhu AX (2007) Advanced hepatocellular carcinoma: CT perfusion of liver and tumor tissue—initial experience. *Radiology* 243:736–743
2. Cuenod C, Leconte I, Siauve N, et al. (2001) Early changes in liver perfusion caused by occult metastases in rats: detection with quantitative CT. *Radiology* 218:556–561
3. Cenic A, Nabavi DG, Craen RA, Gelb AW, Lee TY (1999) Dynamic CT measurement of cerebral blood flow: a validation study. *AJNR Am J Neuroradiol* 20:63–73
4. Nagamachi S, Czernin J, Kim AS, et al. (1996) Reproducibility of measurements of regional resting and hyperemic myocardial blood flow assessed with PET. *J Nucl Med* 37:1626–1631
5. Smith AM, Grandin CB, Duprez T, Maigne F, Cosnard G (2000) Whole brain quantitative CBF, CBV, and MTT measurements using MRI bolus tracking: implementation and application to data acquired from hyperacute stroke patients. *J Magn Reson Image* 12:400–410
6. Jerosch-Herold M, Wilke N, Stillman AE (1998) Magnetic resonance quantification of the myocardial perfusion reserve with a Fermi function model for constrained deconvolution. *Med Phys* 25:73–84
7. Drayer BP, Wolfson SK, Reinmuth OM, et al. (1978) Xenon enhanced CT for analysis of cerebral integrity, perfusion, and blood flow. *Stroke* 9:123–130
8. Meyer JS, Hayman LA, Yamamoto M, Sakai F, Nakajima S (1980) Local cerebral blood flow measured by CT after stable xenon inhalation. *AJR Am J Roentgenol* 135:239–251
9. Sase S, Monden M, Oka H, et al. (2002) Hepatic blood flow measurements with arterial and portal blood flow mapping in the human liver by means of xenon CT. *J Comput Assist Tomogr* 26:243–249
10. Shimizu J, Oka H, Dono K, et al. (2003) Noninvasive quantitative measurement of tissue blood flow in hepatocellular carcinoma using xenon-enhanced computed tomography. *Dig Dis Sci* 48: 1510–1516
11. Murakami T, Hori M, Kim T, et al. (2004) Xenon-inhalation computed tomography for noninvasive quantitative measurement of tissue blood flow in hepatocellular carcinoma. *Invest Radiol* 39:210–215
12. Hashimoto K, Murakami T, Dono K, et al. (2007) Quantitative tissue blood flow measurement of the liver parenchyma: comparison between xenon CT and perfusion CT. *Dig Dis Sci* 52:943–949
13. Willett CG, Boucher Y, di Tomaso E, et al. (2004) Direct evidence that the VEGF-specific antibody bevacizumab has antivascular effects in human rectal cancer. *Nat Med* 10:145–147
14. Ma SH, Le HB, Jia BH, et al. (2008) Peripheral pulmonary nodules: relationship between multi-slice spiral CT perfusion imaging and tumor angiogenesis and VEGF expression. *BMC Cancer* 8:186
15. Li ZP, Meng QF, Sun CH, et al. (2005) Tumor angiogenesis and dynamic CT in colorectal carcinoma: radiologic-pathologic correlation. *World J Gastroenterol* 11:1287–1291
16. Makari Y, Yasuda T, Doki Y, et al. (2007) Correlation between tumor blood flow assessed by perfusion CT and effect of neoadjuvant therapy in advanced esophageal cancers. *J Surg Oncol* 96:220–229
17. Zhu AX, Holalkere NS, Muzikansky A, Horgan K, Sahani DV (2008) Early antiangiogenic activity of bevacizumab evaluated by computed tomography perfusion scan in patients with advanced hepatocellular carcinoma. *Oncologist* 13:120–125
18. Ippolito D, Sironi S, Pozzi M, et al. (2008) Hepatocellular carcinoma in cirrhotic liver disease: functional computed tomography with perfusion imaging in the assessment of tumor vascularization. *Acad Radiol* 15:919–927
19. Llovet JM, Ricci S, Mazzaferro V, et al. (2008) Sorafenib in advanced hepatocellular carcinoma. *N Engl J Med* 359:378–390
20. Bader TR, Herneth AM, Blaicher W, et al. (1998) Hepatic perfusion after liver transplantation: noninvasive measurement with dynamic single-section CT. *Radiology* 209:129–134
21. Hashimoto K, Murakami T, Dono K, et al. (2006) Assessment of the severity of liver disease and fibrotic change: the usefulness of hepatic CT perfusion imaging. *Oncol Rep* 16:677–683

22. Miles KA, Hayball MP, Dixon AK (1993) Functional images of hepatic perfusion obtained with dynamic CT. *Radiology* 188: 405–411
23. Genant HK, Boyd D (1977) Quantitative bone mineral analysis using dual energy computed tomography. *Invest Radiol* 12:545–551
24. Brooks RA (1977) A quantitative theory of the Hounsfield unit and its application to dual energy scanning. *J Comput Assist Tomogr* 1:487–493
25. Nakayama Y, Awai K, Funama Y, et al. (2005) Abdominal CT with low tube voltage: preliminary observations about radiation dose, contrast enhancement, image quality, and noise. *Radiology* 237:945–951
26. Yeh BM, Shepherd JA, Wang ZJ, et al. (2009) Dual-energy and low-kVp CT in the abdomen. *AJR Am J Roentgenol* 193:47–54
27. Graser A, Johnson TR, Bader M, et al. (2008) Dual energy CT characterization of urinary calculi: initial in vitro and clinical experience. *Invest Radiol* 43:112–119
28. Grosjean R, Sauer B, Guerra RM, et al. (2008) Characterization of human renal stones with MDCT: advantage of dual energy and limitations due to respiratory motion. *AJR Am J Roentgenol* 190: 720–728
29. Scheffel H, Stolzmann P, Frauenfelder T, et al. (2007) Dual-energy contrast-enhanced computed tomography for the detection of urinary stone disease. *Invest Radiol* 42:823–829
30. Goldberg HI, Cann CE, Moss AA, et al. (1982) Noninvasive quantitation of liver iron in dogs with hemochromatosis using dual-energy CT scanning. *Invest Radiol* 17:375–380
31. Johnson TR, Krauss B, Sedlmair M, et al. (2007) Material differentiation by dual energy CT: initial experience. *Eur Radiol* 17:1510–1517
32. Primak AN, Fletcher JG, Vrtiska TJ, et al. (2007) Noninvasive differentiation of uric acid versus non-uric acid kidney stones using dual-energy CT. *Acad Radiol* 14:1441–1447
33. Holmes DR 3rd, Fletcher JG, Apel A, et al. (2008) Evaluation of non-linear blending in dual-energy computed tomography. *Eur J Radiol* 68:409–413
34. Behrendt FF, Schmidt B, Plumhans C, et al. (2009) Image fusion in dual energy computed tomography: effect on contrast enhancement, signal-to-noise ratio and image quality in computed tomography angiography. *Invest Radiol* 44:1–6
35. Schindera ST, Nelson RC, Mukundan SJr, et al. (2008) Hypervascular liver tumors: low tube voltage, high tube current multi-detector row CT for enhanced detection—phantom study. *Radiology* 246: 125–132